

Electronic Supplementary Information (ESI)

Experiments

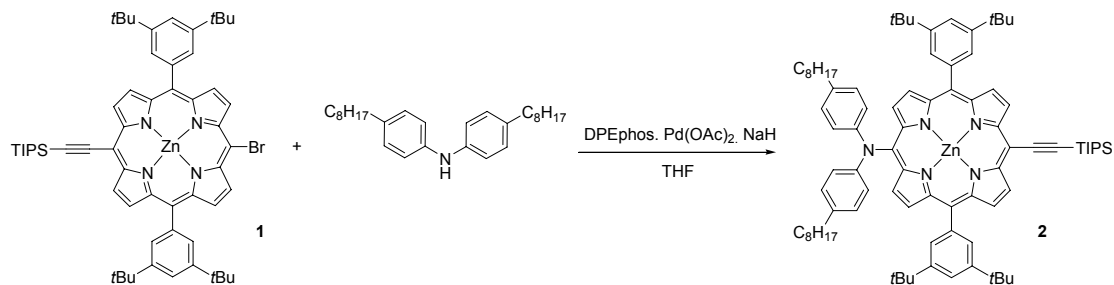
General

All reagents and solvents were obtained from commercial sources and used without further purification unless otherwise noted. CH_2Cl_2 used for electrochemistry was dried over CaH_2 and freshly distilled before use. THF was dried over sodium/benzophenone and freshly distilled before use. Column chromatography was performed on silica gel (Merck, 70-230 Mesh ASTM).

Spectral measurements

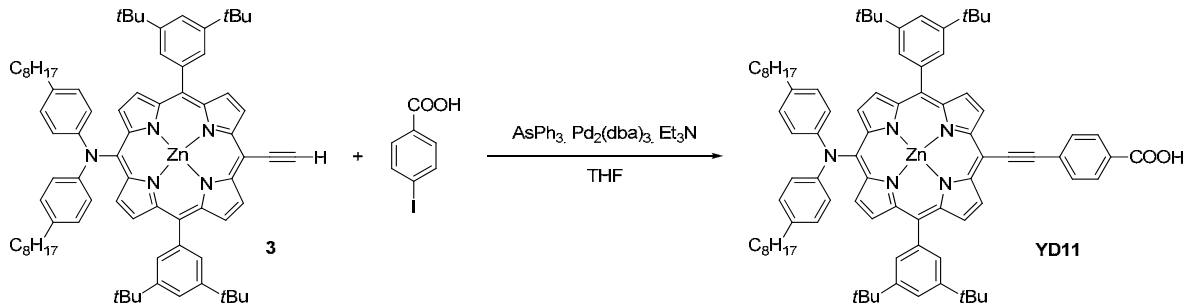
^1H NMR spectra were recorded at 400 MHz, ^{13}C NMR spectra were recorded at 100.56 MHz (Varian spectrometer). UV-Vis spectra were recorded on a spectrometer (Varian Cary 50). FAB-MS mass spectra were obtained from a Tandem Mass spectrometer (JMS-SX/SX102A), operated in the positive-ion detection mode.

Synthetic procedures



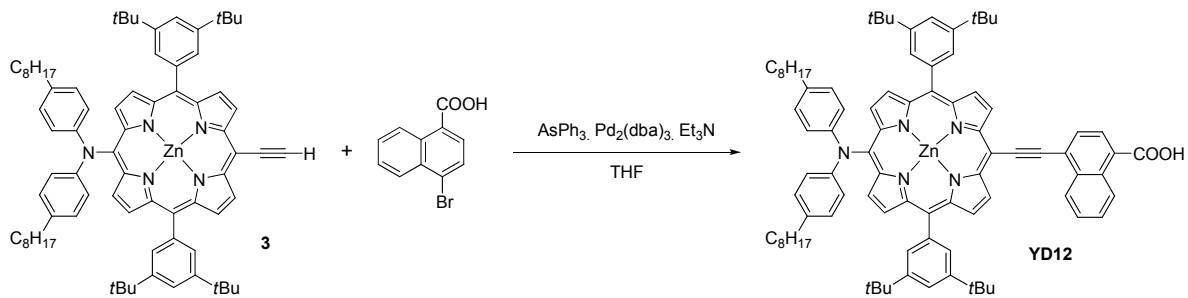
To a degassed solution of bis(4-octylphenyl)amine (200 mg, 0.5 mmol) and 60 % NaH (0.1 mg, 3.96 mmol) in THF (30.0 mL) in a funnel was added porphyrin 1 (200

mg, 0.198 mmol), DPEphos (320 mg, 0.059 mmol), and Pd(OAc)₂ (11 mg, 0.05 mmol). The mixture was refluxed under N₂ for 3 h. The solvent was removed under vacuum and the residue was purified by column chromatography (silica gel) using CH₂Cl₂/hexane = 1/4 as eluent. Recrystallization from CH₂Cl₂/CH₃OH gave **2** (185 mg, 71 %). ¹H NMR (400 MHz, CDCl₃) δ_H = 9.75 (d, *J* = 4.8 Hz, 2H), 9.23 (d, *J* = 4.8 Hz, 2H), 8.95 (d, *J* = 4.8 Hz, 2H), 8.81 (d, *J* = 4.8 Hz, 2H), 8.00 (d, *J* = 1.6 Hz, 4H), 7.78 (t, *J* = 1.6 Hz, 2H), 7.23 (d, *J* = 8.8 Hz, 4H), 6.98 (d, *J* = 8.8 Hz, 4H), 2.49 (t, *J* = 7.6 Hz, 4H), 1.52 (s, 36H), 1.27 (m, 22H), 0.85 (m, 8H) ppm; ¹³C NMR (100.56 MHz, CDCl₃) δ_C = 152.7, 152.5, 150.6, 150.5, 149.9, 148.7, 141.3, 134.9, 133.2, 133.1, 130.8, 130.7, 129.4, 128.9, 124.0, 123.1, 122.1, 121.0, 109.6, 100.5, 97.6, 35.2, 35.0, 31.9, 31.8, 31.5, 29.4, 29.3, 29.2, 22.6, 19.1, 14.1, 11.9 ppm; UV-vis (CH₃CH₂OH): λ_{max}/nm (rel. int.) = 430 (1.00), 583 (0.11), 639 (0.16); MS(FAB): *m/z* 1322 u (MH⁺) calculated for C₈₇H₁₁₃N₅Si Zn 1321 u.



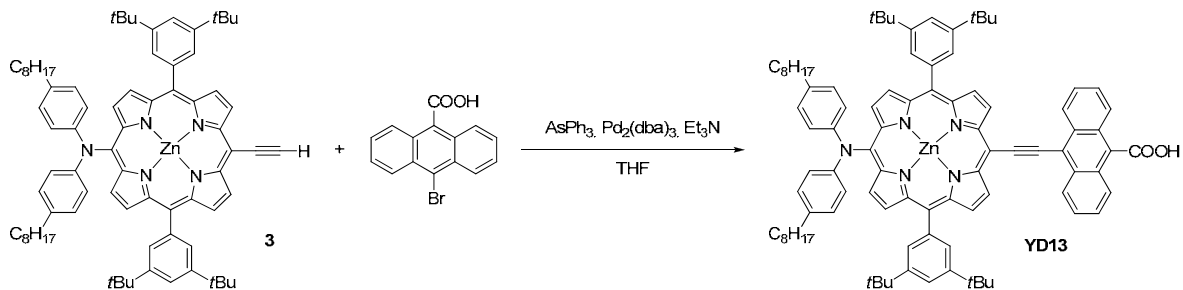
To a solution of porphyrin **2** (150 mg, 0.113 mmol) in THF (23 mL) was added TBAF (0.2 mL, 1 M in THF). The solution was stirred near 23 °C for 30 min under dinitrogen. The solvent was removed under decreased pressure and then extracted with CH₂Cl₂. The organic layer was dried over anhydrous MgSO₄ and the solvent was removed under vacuum. The residue and 4-iodobenzoic acid (130 mg, 0.515 mmol) were dissolved in a mixture of THF (78 mL) and NEt₃ (15 mL) and degassed with

dinitrogen for 10 min; $\text{Pd}_2(\text{dba})_3$ (35.3 mg, 0.039 mmol) and AsPh_3 (100 mg, 0.322 mmol) were added to the mixture. The solution was refluxed under N_2 for 3 h and the solvent was removed under vacuum. The residue was purified by column chromatography (silica gel) using CH_2Cl_2 /methanol = 95/5 as eluent. Recrystallization from $\text{CH}_2\text{Cl}_2/\text{CH}_3\text{OH}$ gave **YD11** (120 mg, 93 %). ^1H NMR (400 MHz, CDCl_3) $\delta_{\text{H}} =$ 9.78 (d, $J = 4.8$ Hz, 2H), 9.29 (d, $J = 4.8$ Hz, 2H), 9.00 (d, $J = 4.8$ Hz, 2H), 8.83 (d, $J = 4.8$ Hz, 2H), 8.24 (d, $J = 8.4$ Hz, 2H), 8.11 (d, $J = 8.4$ Hz, 2H), 8.04 (d, $J = 1.6$ Hz, 4H), 7.80 (t, $J = 1.6$ Hz, 2H), 7.23 (d, $J = 8.8$ Hz, 4H), 6.99 (d, $J = 8.8$ Hz, 4H), 2.49 (t, $J = 7.6$ Hz, 4H), 1.54 (s, 36H), 1.25 (m, 22H), 0.85 (m, 8H) ppm; ^{13}C NMR (100.56 MHz, CDCl_3) $\delta_{\text{C}} =$ 152.6, 152.3, 150.5, 150.5, 150.1, 148.8, 141.1, 135.0, 134.1, 133.4, 131.4, 130.0, 123.6, 122.1, 121.1, 99.2, 96.5, 95.5, 35.1, 31.9, 31.8, 31.5, 29.3, 29.4, 29.2, 22.6, 14.1 ppm; UV-vis ($\text{CH}_3\text{CH}_2\text{OH}$): λ_{max} /nm (rel. int.) = 442 (1.00), 587 (0.09), 646 (0.19); MS(FAB): m/z 1286 u (MH^+) calculated for $\text{C}_{85}\text{H}_{97}\text{N}_5\text{O}_2\text{Zn}$ 1285 u.



To a degassed solution of porphyrin **3** (80 mg, 0.069 mmol) and 4-bromo-1-naphthoic acid (172 mg, 0.69 mmol) in a mixture of THF (42 mL) and NEt_3 (8.2 mL) was added $\text{Pd}_2(\text{dba})_3$ (18.8 mg, 0.021 mmol) and AsPh_3 (52 mg, 0.172 mmol). The mixture was refluxed under N_2 for 10 h and the solvent was removed under vacuum. The residue was purified by column chromatography (silica gel) using CH_2Cl_2 /methanol = 95/5 as eluent. Recrystallization from $\text{CH}_2\text{Cl}_2/\text{CH}_3\text{OH}$ gave **YD12** (68 mg, 74%). ^1H

NMR (400 MHz, CDCl₃) δ_H = 9.87 (d, *J* = 4.4 Hz, 2H), 9.31 (d, *J* = 8.0 Hz, 1H), 9.22 (m, 3H), 8.96 (d, *J* = 4.4 Hz, 2H), 8.75 (d, *J* = 4.4 Hz, 2H), 8.51 (d, *J* = 7.6 Hz, 1H), 8.31 (d, *J* = 7.6 Hz, 1H), 7.99 (d, *J* = 1.6 Hz, 4H), 7.85 (m, 2H), 7.78 (t, *J* = 1.6 Hz, 2H), 7.19 (d, *J* = 8.8 Hz, 4H), 6.94 (d, *J* = 8.8 Hz, 4H), 2.48 (t, *J* = 7.6 Hz, 4H), 1.52 (s, 36H), 1.27 (m, 22H), 0.86 (m, 8H) ppm; ¹³C NMR (100.56 MHz, CDCl₃) δ_C = 170.3, 152.3, 150.6, 150.3, 149.5, 149.2, 148.9, 148.4, 141.7, 135.6, 135.4, 135.2, 134.6, 129.8, 128.9, 123.4, 123.2, 123.1, 122.9, 121.9, 120.7, 98.7, 93.9, 35.2, 34.9, 31.8, 31.7, 31.4, 29.4, 29.2, 22.6, 13.9 ppm; UV-vis (CH₃CH₂OH) : λ_{max}/nm (rel. int.) = 449 (1.00), 588 (0.09), 650 (0.22); MS(FAB): *m/z* 1336 u (MH⁺) calculated for C₈₉H₉₉N₅O₂ Zn 1335 u.



To a degassed solution of porphyrin **3** (80 mg, 0.069 mmol) and 10-bromoanthracene-9-carboxylic acid (210 mg, 0.69 mmol) in a mixture of THF (42 mL) and NEt₃ (8.2 mL) were added Pd₂(dba)₃ (18.8 mg, 0.021 mmol) and AsPh₃ (52 mg, 0.172 mmol). The solution was refluxed under N₂ for 10 h and the solvent was removed under vacuum. The residue was purified on a column chromatograph (silica gel) using CH₂Cl₂/methanol = 95/5 as eluent. Recrystallization from CH₂Cl₂ /CH₃OH gave **YD13** (65 mg, 68 %). ¹H NMR (400 MHz, CDCl₃) δ_H = 9.96 (d, *J* = 4.4 Hz, 2H), 9.35 (d, *J* = 8.4 Hz, 2H), 9.18 (d, *J* = 4.4 Hz, 2H), 8.96 (d, *J* = 4.4 Hz, 2H), 8.73 (d, *J* = 4.4 Hz, 2H), 8.44 (d, *J* = 8.4 Hz, 2H), 7.97 (d, *J* = 1.6 Hz, 4H), 7.68 (s, 4H), 7.63 (m, 2H), 7.17 (d, *J*

= 8.4 Hz, 4H), 6.91 (d, J = 8.4 Hz, 4H), 2.45 (t, J = 7.6 Hz, 4H), 1.48 (s, 36H), 1.22 (m, 22H), 0.82 (m, 8H) ppm; ^{13}C NMR (100.56 MHz, CDCl_3) δ_{C} = 152.3, 152.2, 150.6, 150.2, 149.4, 149.1, 148.8, 148.3, 135.6, 135.3, 135.1, 134.5, 133.6, 129.5, 128.6, 123.3, 123.2, 123.0, 122.8, 121.8, 120.7, 35.1, 34.9, 31.7, 31.6, 31.4, 29.6, 29.3, 29.2, 29.1, 22.5, 13.9 ppm; UV-vis ($\text{CH}_3\text{CH}_2\text{OH}$) : $\lambda_{\text{max}}/\text{nm}$ (rel. int.) = 476 (1.00), 588 (0.11), 660 (0.29); MS(FAB): m/z 1386 u (MH^+) calculated for $\text{C}_{93}\text{H}_{101}\text{N}_5\text{O}_2\text{Zn}$ 1385 u.

Electrode preparation and device fabrication

The photoanodes composed of nanocrystalline TiO_2 were prepared using the sol-gel method reported elsewhere.⁹ A paste composed of about 20-nm TiO_2 particles for the transparent nanocrystalline layer was coated on a TiCl_4 -treated FTO glass substrate (FTO, 30 Ω/\square) to obtain the required thickness by repetitive screen printing. To improve the performance of DSSC, one additional scattering layer (particle size 200–600 nm) was screen-printed on the transparent nanocrystalline layer; the corresponding SEM images for films A ($L \sim 5 \mu\text{m}$), B ($L \sim 10 \mu\text{m}$), and C ($L \sim (10+4) \mu\text{m}$) are shown in Fig. S2. The TiO_2 working electrodes were gradually heated according to a programmed procedure: (1) heating at 80 °C for 15 min; (2) heating at 135 °C for 10 min; (3) heating at 325 °C for 30 min; (4) heating at 375 °C for 5 min; (5) heating at 450 °C for 15 min; (6) heating at 500 °C for 15 min. After cooling in air, the sintered TiO_2 films were immersed in dye solutions (for **YD11-YD13**: 0.2 mM in anhydrous ethanol at 25 °C for 12 h; for **N719**: 0.3 mM in 1:1 (v/v) acetonitrile and *tert*-butanol at 25 °C for 18 h) containing CDCA (0.3 mM for **N719**, 0 or 0.4 mM for **YD11-YD13** as noted in the text) for dye loading onto the working electrodes. The counter electrode was made by spin-coating the H_2PtCl_6 /isopropanol solution onto an indium-doped tin oxide (ITO; 5.5 Ω/\square) glass substrate (typical size $1.0 \times 1.5 \text{ cm}^2$) through thermal

decomposition at 380 °C for 30 min. The two electrodes were assembled into a cell of sandwich type and sealed with a hot-melt film (SX1170, thickness 25 µm). The electrolyte solution for **YD11-YD13** devices contains LiI (0.1 M), I₂ (0.05 M), PMII (0.6 M) and 4-*tert*-butylpyridine (0.5 M) in a solvent mixture containing acetonitrile and valeronitrile (volume ratio 1:1),^{4d} whereas that for the N719 device contains LiI (0.05 M), I₂ (0.03 M), DMII (1.0 M), 4-*tert*-butylpyridine (0.5 M) and GuNCS (0.1 M) in a solvent mixture containing acetonitrile and valeronitrile (volume ratio 85:15).^{2c}

Dye-loading examination

To determine the dye-loading amount of the **YD11-YD13** on TiO₂ films, the dye was desorbed in tetrabutylammonium hydroxide (0.1 M, TBA, Fluka) in ethanol (3 mL). The absorption spectrum of the solution was recorded with a UV-vis spectrometer (Varian, Cary 50). A calibration curve for **YD11-YD13** in ethanol was derived to obtain the absorption coefficient shown in Figure 1. The amounts of dye coverage on TiO₂ films shown in Table 1 were obtained from the measured absorbances in the spectra (cuvette thickness 1 mm) and the calibrated absorption coefficient of **YD11-YD13** according to Beers' law. A similar method was used to determine the dye-loading amount of **N719** on TiO₂ films, but the dye was desorbed in NaOH aqueous solution (0.1 M).

Photovoltaic characterization

The current-voltage characteristics were determined with a digital source meter (Keithley 2400, computer-controlled) with the device under one-solar AM 1.5 irradiation from a solar simulator (SAN-EI, XES-502S) calibrated with a standard silicon reference cell (VLSI standards, Oriel PN 91150V). When the device is

irradiated with the solar simulator, the source meter sends a voltage (V) to the device, and the photocurrent (I) is read at each step controlled with a computer via a GPIB interface. The efficiency (η) of conversion of light to electricity is obtained with these relations, $\eta = J_{sc} V_{oc} \text{FF} / P_{in}$, in which J_{sc} /mA cm $^{-2}$ is the current density measured at short circuit, and V_{oc} /V is the voltage measured at open circuit. P_{in} is the input radiation power (for one-sun illumination $P_{in} = 100$ mW cm $^{-2}$) and FF is the fill factor. For all measurements, the DSSC devices were covered with a black mask of aperture area 0.16 cm 2 to ensure the measured photocurrent not being exaggerated. The spectra of the incident photons-to-current conversion efficiency (IPCE) of the corresponding devices were obtained with a system comprising a Xe lamp (PTi A-1010, 150 W), a monochromator (Dongwoo DM150i, 1200 gr/mm blazed at 500 nm), and a source meter (Keithley 2400). A standard Si photodiode (ThorLabs FDS1010) served as a reference to calibrate the power density of the light source at each wavelength. Both photocurrent densities of the target device and the reference Si cell were measured under the same experimental conditions (excitation beam size ~0.08 cm 2) so to obtain the efficiency of the device from a comparison of the current ratio and the value of the reference cell at each wavelength.¹⁰

Femtosecond fluorescence up-conversion

Fluorescence decays were recorded with an optically gated up-conversion system (FOG100, CDP), described elsewhere.^{5b} Briefly, the femtosecond laser system (Mira 900D, Coherent) generated output pulses at 860 nm of duration ~120 fs at a repetition rate 76 MHz. The frequency of the laser pulse was doubled for excitation ($\lambda_{ex} = 430$ nm). The residual fundamental pulse served as an optical gate; a dichroic beam splitter separated excitation and gate beams. The intensity of the excitation beam was

appropriately attenuated and focused onto a rotating cell (optical path of length 1 mm) containing the thin-film samples. The emission was collected with two parabolic mirrors and focused onto a crystal (BBO type-I); the gate pulse was also focused on that BBO crystal for sum-frequency generation. The latter signal was collected with a lens, and separated from interference light with an iris, a band-pass filter, and a double monochromator (DH10, Jobin Yvon) in combination, then detected with a photomultiplier (R1527P, Hamamatsu) connected to a computer-controlled photon-counting system. On varying the temporal delay between gate and excitation pulses via a stepping-motor translational stage, we obtained a temporal profile. To prepare a thin-film sample, we screen-printed nanocrystalline TiO₂ and Al₂O₃ films on glass substrates with active size 1.0 × 1.0 cm². Nanocrystalline films were soaked in a porphyrin/ethanol solution (2×10^{-4} M) until the absorbance of the films at the Q-band attained 0.5 (Figure S4).

Supplementary Tables

Table S1. Absorption, fluorescence and electrochemical data for **YD11-YD13**.^a

Porphyrins	Absorption $\lambda_{\text{max}}[\text{nm}]$	Emission $\lambda_{\text{max}}[\text{nm}]$	Oxidation $E_{1/2} / \text{V}$	Reduction $E_{1/2} / \text{V}$
YD11	442, 587, 646	674 ^b	+0.91, +1.29 ^c	-1.09
YD12	449, 588, 650	679 ^b	+0.92, +1.30 ^c	-1.15 ^c
YD13	476, 588, 660	689 ^b	+0.90, +1.26 ^c	-1.20 ^c

^a Absorption and emission data were measured in ethanol for **YD11-YD13** at 298 K. Electrochemical measurements were performed at 25 °C in THF containing TBAPF₆ (0.1 M) as supporting electrolyte. Potentials measured vs ferrocene/ferrocenium (Fc/Fc⁺) couple were converted to normal hydrogen electrode (NHE) by addition of +0.63 V.^{S1} ^b The excitation wavelength was 600 nm. ^c Irreversible process E_{pa} or E_{pc} .

- S1. D. P. Hagberg, J.-H. Yum, H. Lee, F. D. Angelis, T. Marinado, K. M. Karlsson, R. Humphry-Baker, L. Sun, A. Hagfeldt, M. Grätzel, M. K. Nazeeruddin, *J. Am. Chem. Soc.*, **2008**, 130, 6259-6266.

Table S2. Photovoltaic parameters of DSSC with photosensitizers **YD11-YD13** and **N719** at TiO₂ film thickness of ~5 μm (Film A)^a under simulated AM-1.5 illumination (power 100 mW cm⁻²) and active area 0.16 cm².

Dye	Working Electrode	J_{SC} /mA cm ⁻²	V_{OC} /V	FF	η /%
YD11	a	10.53	0.724	0.73	5.57
	b	10.60	0.724	0.73	5.60
	c	10.31	0.730	0.73	5.49
	d	10.70	0.714	0.72	5.50
average		10.54±0.33	0.723±0.013	0.73±0.01	5.54±0.11
YD12	a	10.76	0.725	0.72	5.62
	b	10.61	0.725	0.72	5.54
	c	10.64	0.727	0.73	5.65
	d	10.98	0.717	0.71	5.59
average		10.75±0.34	0.724±0.009	0.72±0.02	5.60±0.09
YD13	a	3.40	0.636	0.71	1.54
	b	3.29	0.629	0.72	1.49
	c	3.20	0.633	0.71	1.44
	d	3.29	0.634	0.71	1.48
average		3.30±0.16	0.633±0.006	0.71±0.01	1.49±0.08
N719	a	9.17	0.795	0.75	5.47
	b	9.28	0.796	0.74	5.47
	c	9.31	0.790	0.74	5.44
	d	9.31	0.796	0.74	5.48
average		9.27±0.13	0.794±0.006	0.74±0.01	5.47±0.03

a All the TiO₂ working electrodes (labeled as a-d) were fabricated under the same experimental conditions.

Table S3. Photovoltaic parameters of DSSC with photosensitizers **YD11-YD13** and **N719** at TiO₂ film thickness of ~10 µm (Film B)^a under simulated AM-1.5 illumination (power 100 mW cm⁻²) and active area 0.16 cm².

Dye	Working Electrode	J_{SC} /mA cm ⁻²	V_{OC} /V	FF	η /%
YD11	a	13.42	0.714	0.69	6.61
	b	12.96	0.713	0.71	6.56
	c	12.59	0.719	0.72	6.52
	average	12.99±0.83	0.715±0.006	0.71±0.03	6.56±0.09
YD12	a	13.78	0.714	0.68	6.69
	b	13.83	0.716	0.68	6.73
	c	13.96	0.716	0.67	6.70
	d	13.49	0.711	0.69	6.62
	average	13.77±0.40	0.714±0.005	0.68±0.02	6.69±0.09
YD13	a	3.98	0.618	0.71	1.75
	b	4.01	0.617	0.72	1.78
	c	3.91	0.619	0.72	1.74
	average	3.97±0.10	0.618±0.002	0.72±0.01	1.76±0.04
N719	a	10.92	0.768	0.73	6.12
	b	11.28	0.770	0.72	6.25
	c	10.83	0.770	0.74	6.17
	d	10.85	0.769	0.73	6.09
	average	10.97±0.42	0.769±0.002	0.73±0.02	6.16±0.14

a All the TiO₂ working electrodes (labeled as a-d) were fabricated under the same experimental conditions.

Table S4. Photovoltaic parameters of DSSC with photosensitizers **YD11-YD13** and **N719** at TiO₂ film thickness of ~(10+4) μm (Film C)^a under simulated AM-1.5 illumination (power 100 mW cm⁻²) and active area 0.16 cm².

Dye	Working Electrode	J_{SC} /mA cm ⁻²	V_{OC} /V	FF	η /%
YD11	a	13.96	0.716	0.68	6.80
	b	14.09	0.714	0.68	6.84
	c	13.99	0.717	0.67	6.72
	average	14.01±0.14	0.716±0.003	0.68±0.01	6.79±0.12
YD12	a	14.80	0.718	0.66	7.01
	b	14.18	0.713	0.68	6.88
	c	13.83	0.722	0.69	6.89
	d	14.09	0.714	0.68	6.84
	average	14.23±0.82	0.717±0.008	0.68±0.03	6.91±0.15
YD13	a	4.10	0.631	0.71	1.84
	b	4.16	0.629	0.72	1.88
	c	4.09	0.630	0.72	1.86
	average	4.12±0.08	0.630±0.002	0.72±0.01	1.86±0.04
N719	a	13.13	0.781	0.71	7.28
	b	13.23	0.789	0.70	7.31
	c	13.10	0.787	0.71	7.32
	d	12.86	0.785	0.71	7.17
	average	13.08±0.31	0.786±0.007	0.71±0.01	7.27±0.14

a All the TiO₂ working electrodes (labeled as a-d) were fabricated under the same experimental conditions.

Table S5. Comparison of photovoltaic parameters of **YD11-YD13** devices under simulated AM-1.5 illumination (power 100 mW cm⁻²) obtained from analysis of *J-V* curves of Figure S5.

Dye	[Dye]:[CDCA]	Dye-loading /nmol cm ⁻²	<i>J_{SC}</i> /mA cm ⁻²	<i>V_{OC}</i> /V	FF	η /%
YD11	1 : 0	145	13.43	0.714	0.69	6.62
	1 : 2	134	13.17	0.721	0.69	6.55
YD12	1 : 0	153	13.68	0.718	0.68	6.68
	1 : 2	131	13.40	0.718	0.68	6.54
YD13	1 : 0	135	4.22	0.631	0.71	1.89
	1 : 2	126	6.27	0.652	0.71	2.90

Supplementary Graphics

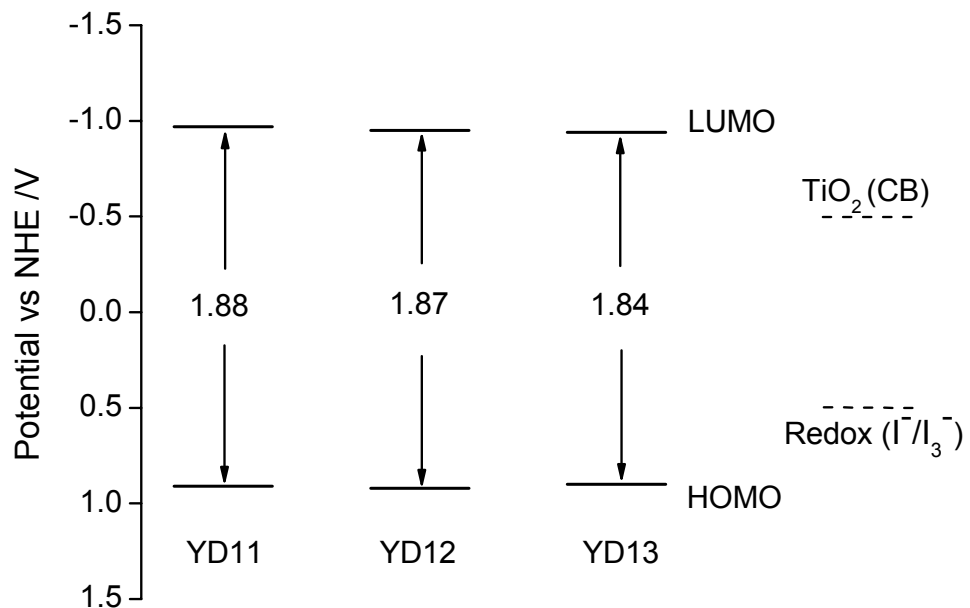


Figure S1. Energy-level diagram of YD11-YD13 showing the HOMO and the LUMO of each porphyrin. The energy levels of the HOMO were determined from electrochemical data (oxidation potentials) and those of the LUMO were determined from spectral data (band gaps).

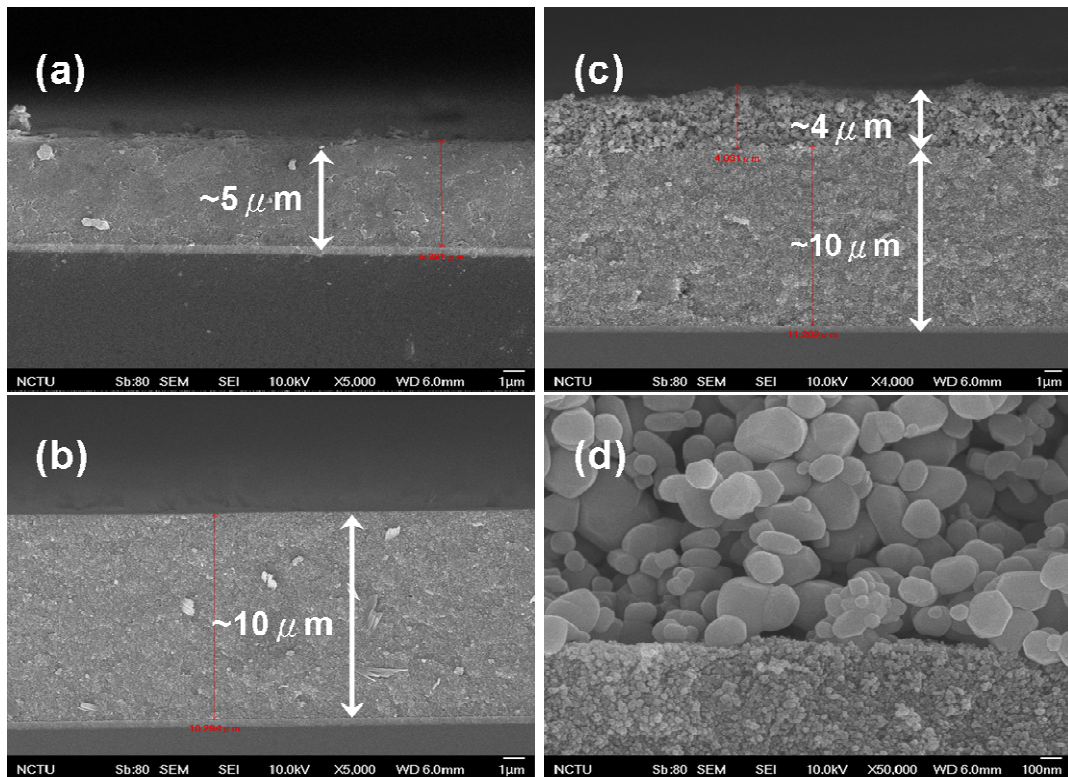


Figure S2. SEM images of TiO_2 films of three types used in the present work: (a) $L \sim 5 \mu\text{m}$ (film A); (b) $L \sim 10 \mu\text{m}$ (film B); (c) $L \sim(10+4) \mu\text{m}$ (film C); (d) enlarged side view of the SEM image of (c) showing the interface between the active layer (particle size $\sim 20 \text{ nm}$) and the scattering layer (particle size $200\text{-}600 \text{ nm}$).

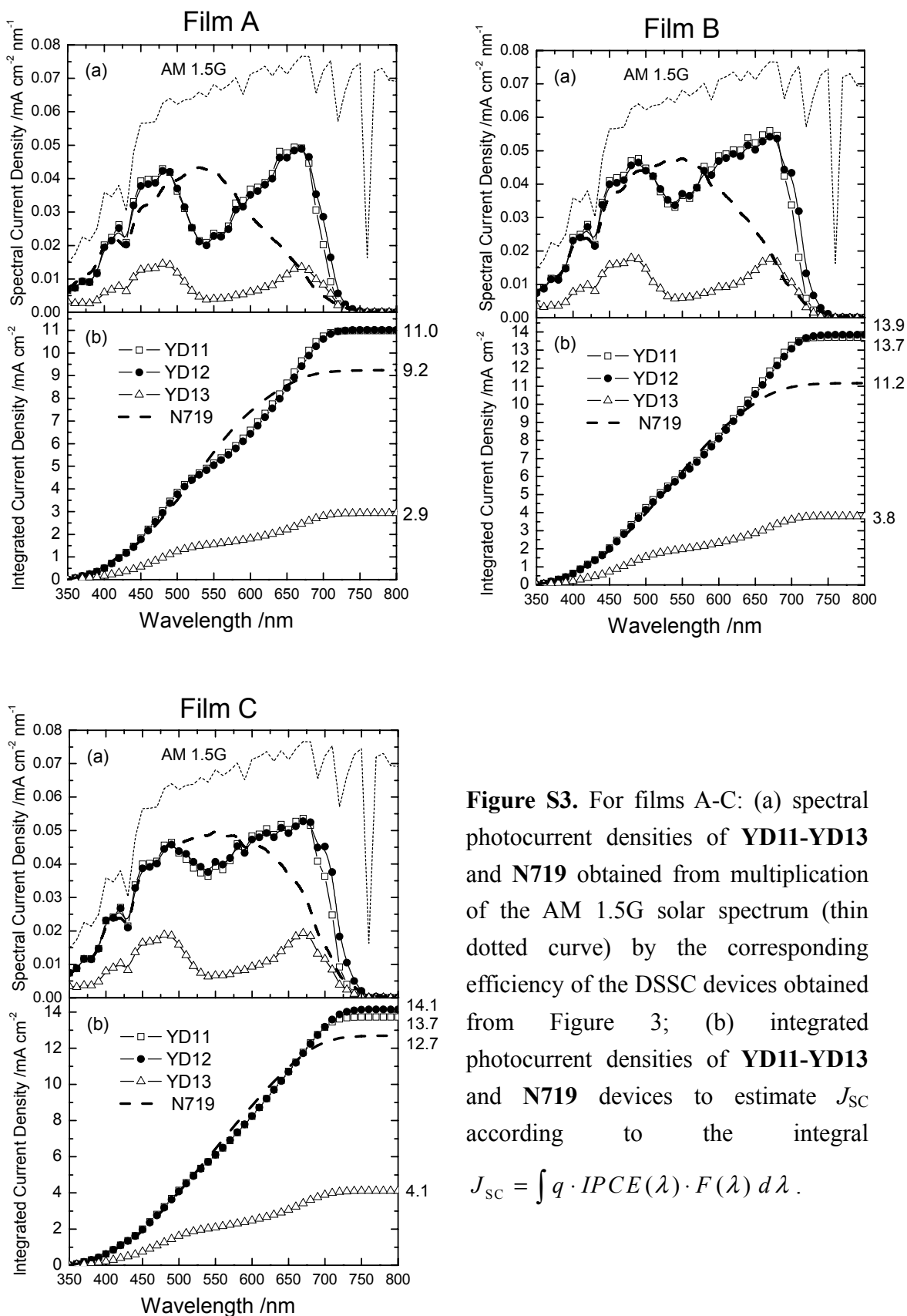


Figure S3. For films A-C: (a) spectral photocurrent densities of **YD11-YD13** and **N719** obtained from multiplication of the AM 1.5G solar spectrum (thin dotted curve) by the corresponding efficiency of the DSSC devices obtained from Figure 3; (b) integrated photocurrent densities of **YD11-YD13** and **N719** devices to estimate J_{SC} according to the integral

$$J_{SC} = \int q \cdot IPCE(\lambda) \cdot F(\lambda) d\lambda .$$

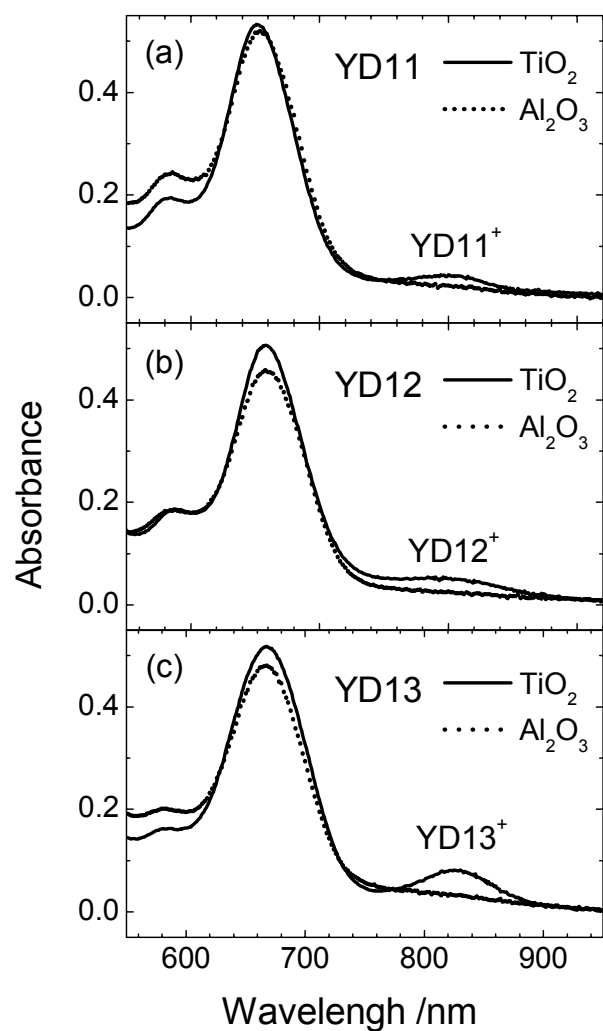


Figure S4: Absorption spectra of (a) YD11, (b) YD12, and (c) YD13 sensitized on TiO_2 (solid traces) and Al_2O_3 films (dotted traces). The absorption bands ~ 800 nm were due to the formation of cationic species upon photoexcitation.

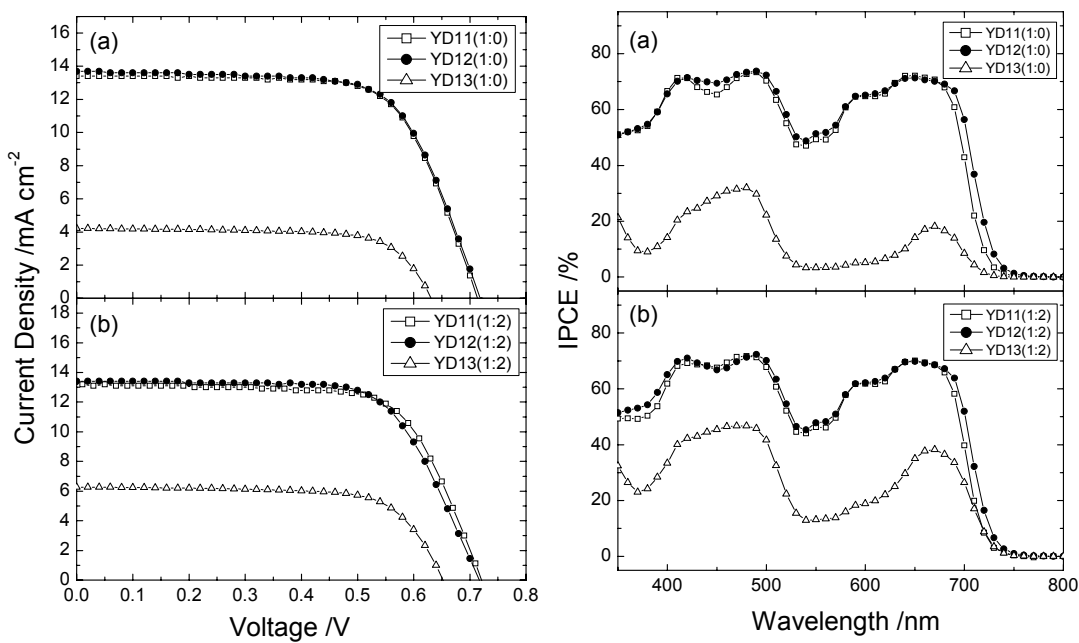


Figure S5. (Left) Current-voltage characteristics of DSSC devices with sensitizers of **YD11-YD13** and film thicknesses $\sim 10 \mu\text{m}$ (film B) under illumination of simulated AM1.5 full sunlight (100 mW cm^{-2}) for (a) without and (b) with added CDCA co-sensitizer ($[\text{dye}]:[\text{CDCA}] = 1:2$) ; (Right) corresponding IPCE action spectra.